

# Reactive Power and Energy Instrument's Performance in Non-Sinusoidal Conditions Regarding Different Power Theories

Kiril Demerdziev\*, Vladimir Dimchev

*Institute of Electrical Measurements and Materials, Faculty of Electrical Engineering and Information Technologies (FEEIT), Ss. Cyril and Methodius University in Skopje (UKIM), st. "Rugjer Boskovic" No.18, Skopje, North Macedonia, [kdemerdziev@feit.ukim.edu.mk](mailto:kdemerdziev@feit.ukim.edu.mk), [vladim@feit.ukim.edu.mk](mailto:vladim@feit.ukim.edu.mk)*

**Abstract:** It is important to conduct the examination of reactive power and energy instruments in normal operating conditions, due to their place in the regulated trade of electrical energy. The challenge arises when the normal operating conditions encompass non-sinusoidal voltages and currents, for two main reasons: the fact that the term reactive power/energy is not unambiguously defined in case of harmonically polluted environment and the fact that the measurement algorithm implemented in the meter is usually not explicitly presented by the producer. Different algorithms provide the same result in case of sinusoidal signals, while in case of harmonics the instrument's performance may vary significantly, when different power theories are adopted. In the paper, a commercially available reactive energy electricity meter is tested with harmonically distorted voltage and current signals, and an analysis of its output is performed from the perspective of the implemented measuring algorithm, which is not known a priori. The tests encompass alteration of different waveform parameters and the instrument's output is analyzed from the perspective of several reactive power theories. The conclusion of the analysis results in the meter's performance feature illustration in correlation with different harmonic parameters and different reference conditions.

**Keywords:** High order harmonics, phase shifts, reactive power theories, measurement algorithm error curves, electricity meter.

## 1. INTRODUCTION

The harmonic distortion of voltage and current signals denotes that demands for accurate measurement in power systems at any voltage level go beyond the instruments' specifications, which refer to reference sine-wave conditions. This is especially important in the field of legal metrology, i.e., when considering electricity meters, because of their billing role in the regulated trade of electrical energy. According to EU Directive MID 2014/32/EU [1] "all measuring instruments used for commercial transactions" are supposed to measure the quantity of particular interest with "error which will not exceed the maximal permissible error under rated operating conditions". The maximal permissible error is "the extreme value of measurement error, with respect to a known reference quantity value, permitted by specifications or regulations for a given measurement, measuring instrument or measuring system" [2]. In case of harmonically distorted waveforms, the maximal permissible error of a measuring instrument is not limited only by its accuracy class, but possesses an additional component due to the distortion conditions. The rated operating conditions are "operating condition that must be fulfilled during

measurement in order for a measuring instrument or a measuring system to perform as designed" and they do not longer encompass only pure sinusoidal voltages and currents, but harmonically polluted waveforms as well [2]-[3].

In the domain of active electricity meter testing, several international standards [4]-[6], a recommendation [2], and plenty of scientific works [7]-[14] exist, and therefore different examination protocols are established. In the EN 50470-3 standard [6], signals that possess the 5th order harmonics, beside fundamental voltages and currents, are proposed as test conditions for calibration of active electricity meters in non-sinusoidal environment. The share of the 5th order voltage harmonic equals 10% of the voltage fundamental, while the 5th order current harmonic equals 40% of the current fundamental. Both voltage and current harmonics are in phase with the 50 Hz components at positive zero crossing. Test signals with similar limitation for the harmonic distortion are presented in OIML R 46-1/-2 Recommendation [2]. In this document, two test signals that encompass odd harmonics up to the 13th order are proposed, called Quadriform and Peaked waveform. The harmonic components are either in phase with fundamentals or they are 180° phase shifted. In the considered scientific papers [7]-

[14], examination protocols that encompass multiple harmonic components with random share and phase shifts are also presented. In these papers, instruments' performance is regarded in accordance with: the degree of harmonic distortion [8], the load balance [7], the duration of the disturbances [9], and the single harmonic parameters' values [12], [14].

On the other hand, no test procedures are proposed for reactive electricity meter examination. The main reason for that is the fact that the term reactive power/energy is not unambiguously defined in harmonically polluted environment [3], [15]. Several reactive power definitions in case of non-sinusoidal waveforms exist, each one possesses certain advantages and flaws. The second reason for the lack of standardized calibration procedure existence are the different measuring algorithms, on which different instruments are based. All the existing algorithms provide the same result in case of sinusoidal voltages and currents, but the outcome is different in case of harmonically polluted input signals [3]. In the EN 62053-23 standard [16], accuracy demands for reactive electricity meters are presented, but they are limited to sine-wave conditions. A progress with understanding and unification of the reactive power/energy measurements was made with the publication of the IEEE 1459 standard [17], in which it is stated that the quantity of particular interest for accurate measurement is the fundamental reactive power, Q1. The main drawback of Q1 only measurement is that it does not provide equality in terms of billing penalization of distortion producers and consequently, billing compensation of the harmonics consumers [18].

Considering all pre-mentioned complications, an analysis of a commercially available reactive energy electricity meter's output, in harmonically polluted environment, will be performed. The Unit Under Test (UUT) will be examined with a Reference Standard (RS) that is suitable for both reproducing harmonically distorted voltages and currents, and determining the output reference reactive power/energy, according to a different power definition. The difference between the measured and the generated power is regarded only from the UUT's measurement algorithm perspective, i.e., no additional analysis of the single harmonics' impact on constructive parts of the meter is performed. The main contribution of the work is related to the determination of the measurement capabilities of UUT, when different distortions of the voltage and current signals are present, in relation to different reactive power theories. By performing such an analysis, the measurement algorithm, which is not presented a priori by the producer, may also be determined. Because no test signals are provided in the cited standards, a starting point for the concrete analysis are the waveforms presented in [6], intended for active electricity meter examination in non-sinusoidal conditions. Multiple tests are performed by altering different harmonic and fundamental parameters of the test waveforms.

## 2. BASIC MATHEMATICS IN HARMONIC ANALYSIS

A harmonically distorted voltage or current signal is mathematically evaluated by using Fourier series [19]-[21]:

$$x(t) = \sqrt{2} \sum_{h=1}^n X_h \sin(h\omega t + \alpha_{xh}), \quad (1)$$

where  $x(t)$  is the time-domain representation of the voltage or current signal,  $h$  is the harmonic order,  $\omega$  is the angular frequency,  $X_h$  and  $\alpha_{xh}$  are the RMS and the initial phase shift of the component with a frequency  $h$  times the fundamental and  $n$  is the maximal harmonic order which is taken into account for evaluation. The harmonic analysis is usually limited to a 50th component evaluation [20]-[21]. The share of a single harmonic component is commonly expressed as a percentage of the fundamental's value,  $X_1$  [2], [6]-[9], [14]:

$$x_h [\%] = \frac{X_h}{X_1} \cdot 100, \quad (2)$$

while its phase shift is presented in relation to the initial phase shift of a 50 Hz component, at positive zero crossing,  $\alpha_{x1}$ :

$$\theta_{xh} = \alpha_{xh} - \alpha_{x1}. \quad (3)$$

The single phase active power, in case of harmonically distorted waveforms, is expressed as a mean power in a pre-defined time period,  $T$  [7], [9], [14], [22]:

$$P = \frac{1}{T} \int_0^T u(t)i(t) dt = \sum_{h=1}^n P_h = \sum_{h=1}^n U_h I_h \cos \varphi_h, \quad (4)$$

and it equals the algebraic sum of the active power components obtained from the voltages and currents at different frequencies. In (4),  $U_h$  and  $I_h$  are the RMS values of the voltage and current harmonics of order  $h$  and they can be mathematically evaluated using (2), if the percentage shares,  $u_h[\%]$  and  $i_h[\%]$ , and fundamental RMS values,  $U_1$  and  $I_1$ , are known. The phase shift between harmonic components of order  $h$ ,  $\varphi_h$ , equals [14], [23]:

$$\varphi_h = h\varphi_1 + \theta_{ih} - \theta_{uh}, \quad (5)$$

$\varphi_1$  being the phase shift between current and voltage at fundamental frequency, while  $\theta_{ih}$  and  $\theta_{uh}$  are the phase shifts between the  $h$ th order current and voltage harmonics and the corresponding components at 50 Hz (3). In (5), the phase shift between fundamentals,  $\varphi_1$ , is multiplied by the harmonic's order  $h$ , because the phasors of harmonic components rotate  $h$  times faster than the phasors of  $U_1$  and  $I_1$  [14].

The single phase apparent power of distorted waveforms equals the product of the signals' RMS values,  $U$  and  $I$  [22]:

$$S = UI = \sqrt{\sum_{h=1}^n U_h^2} \sqrt{\sum_{h=1}^n I_h^2}, \quad (6)$$

and (4) and (6) can be correlated to principles which are valid for both sinusoidal and harmonically distorted conditions. If the P, Q and S triangle, valid for sine-wave signals, is taken as a reference point, the reactive power equals [3], [15]:

$$Q = Q_F = \sqrt{S^2 - P^2}, \quad (7)$$

and this equation derives from the power theory proposed by Fryze, therefore the reactive power is labeled as Fryze power,

QF. According to Fryze, the current signal,  $i(t)$ , is decomposed into two components, called the “active” current,  $i_a(t)$ , which is in phase with the voltage signal and possess the same waveform as  $u(t)$ , and the “non-active” or “reactive” current,  $i_r(t)$ , which is the remaining part of  $i(t)$ . The decomposition of the current signal into 2 components is characterized as a time-domain approach for reactive power clarification [15]. Fryze power is also referred to as “non-active power” and can be further expressed as [24]:

$$Q_F = UI_r, \quad (8)$$

where  $I_r$  is the RMS of the non-active component of the current and  $U$  is the RMS of the distorted voltage signal [15]. The Fryze power theory provides satisfactory explanation of the system’s efficiency and is simple for evaluation using basic phasor knowledge. On the other hand, it cannot be used as a starting point for a compensation solution determination of the system’s reactive power [24].

The other power definition considered in this paper is the one proposed by Budeanu. This power theory is characterized as a frequency-based approach [15]. According to Budeanu, the total reactive power is calculated as an algebraic sum of reactive power components, obtained from ideal sinusoidal waveforms at different frequencies:

$$Q = Q_B = \sum_{h=1}^n Q_h = \sum_{h=1}^n U_h I_h \sin \varphi_h, \quad (9)$$

and it can be fully compensated by using a simple capacitor [24]. If Budeanu’s concept is adopted, then the remaining power, beside  $P$  and  $Q_B$ , is called distortion power,  $D$ :

$$D = \sqrt{S^2 - P^2 - Q_B^2}, \quad (10)$$

and it is the result of the mutual interference between voltages and currents at different frequencies, [15], [20], [22], [24].

As regarded in the IEEE 1459 standard [17], a separation principle between fundamental power and high frequency components is suggested. That is appropriate from the meters’ perspective, because the measuring principle of many instruments used for reactive power or energy monitoring is based on time or phase shift of the voltage or current signal for quarter of a period, or  $90^\circ$ , respectively [3]. As only fundamental reactive power is obtained by quarter period time shifting, or  $90^\circ$  phase shifting of a voltage or current signal, the measured power is expected to equal:

$$Q_1 = U_1 I_1 \sin \varphi_1, \quad (11)$$

where  $U_1$  and  $I_1$  are the RMS of voltage and current at 50 Hz and  $\varphi_1$  is the phase shift between them.

Beside the concepts proposed by Budeanu and Fryze, which are the primary frequency based and time based approaches for reactive power determination in harmonically polluted environment, other power definitions exist as well [15], [24]: Kusters - Moore, Page, Shepard - Zakikhani, Sharon, etc. However, the UUT’s performance in relation to these power definitions is not going to be covered in the practical analysis of this manuscript.

### 3. MEASUREMENT PROCEDURE

The experimental part of the work is performed in an accredited laboratory for calibration of instruments and reference standards for electrical quantities, according to the MKC EN ISO/IEC 17025:2018 standard [25]. It is named Laboratory for Electrical Measurements (LEM) and it is part of the Faculty of Electrical Engineering and Information Technologies (FEEIT) at Ss. Cyril and Methodius University in Skopje (UKIM). The laboratory’s reference standards are periodically calibrated [26]-[27] and maintain international traceability to BIPM. For the purposes of this experiment, LEM’s secondary standard, in the domain of electric power and energy instruments calibrations, CALMET C300 [23] is used as RS. CALMET C300 is a three phase low frequency voltage and current source, which is software controlled and possesses menus for automatic electricity meter calibration. Beside the possibility for pure sine-wave signal generation, the RS reproduces also harmonically distorted waveforms.

The UUT is a commercially available electricity meter for both active and reactive energy, based on Digital Signal Processing (DSP), intended for instrument transformer connection, Landis+Gyr ZMD405CT44.2407, 3x58 V/ 100 V, 5 A, 50 Hz, of accuracy class 1 [28]. In its user manual [28], it is stated that the reactive energy is obtained by  $90^\circ$  phase shifting of the 3 phase voltages, before averaging the sum of products between voltage and current samples over a period of time. No additional information concerning the measurement algorithm, on how the  $90^\circ$  phase shifting of the voltage signals is performed, is presented. The possible implemented solutions will be discussed in the analysis that follows. For simplification of the analysis, measurement made by the UUT’s will be regarded from the perspective of reactive power measurement, rather than from the reactive energy measurement perspective [14].

In Fig. 1, the connection of the UUT to the RS is illustrated. The RS [23] is controlled by a hardware unit, connected via USB/ RS232 interface. Using the software that controls the RS, the harmonic distortion of the voltage and current signals is set in terms of share of single harmonics (2), and their phase shifts in relation to fundamentals (3). The pre-set harmonic distortion is implemented in the measurement procedure, in which measurement points are specified. Beside the measurement points, the power definition, according to which the reference power/energy will be calculated, is also denoted. The pulse output of the UUT is connected to a data acquisition module, as an external conditioning circuit of the RS. The pulses procession, proportional to the measured reactive energy by the UUT, is the input signal into the RS’s pulse input. In such a manner the measured energy is compared to the reference energy, generated by the RS, calculated according to a different power theory. The results are presented in a relative error form:

$$\varepsilon = \frac{W_{UUT} - W_{RS}}{W_{RS}} \cdot 100 \approx \frac{Q_{UUT} - Q_{RS}}{Q_{RS}} \cdot 100, \quad (12)$$

where  $W_{UUT}$  and  $Q_{UUT}$  are the reactive energy and power measured by the UUT, and  $W_{RS}$  and  $Q_{RS}$  are the reactive energy and power generated by the RS.

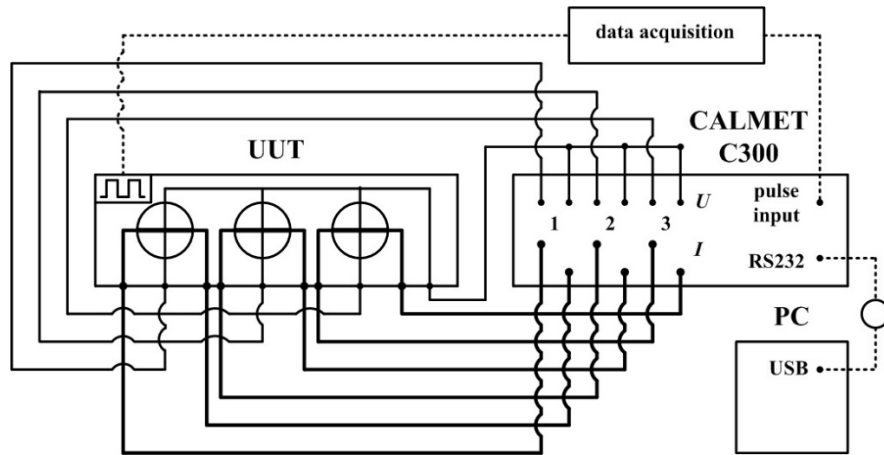


Fig. 1. UUT connection to the CALMET C300 reference standard.

The experimental part of the work is carried out by conducting five measurement procedures. A starting point for their establishment are the test waveforms presented in [6], used for testing of active electricity meters in case of harmonically distorted signals. In each measurement procedure, only one high order harmonic component is present in both voltage and current signals and only one parameter of the harmonics is variable, while all the others are held constant. In 4 out of 5 procedures, test signals, which possess the 5th order harmonics are used. In the last one, the order of the high frequency components, present in the waveforms, is regarded as an influence quantity for determination of the difference between UUT's measurements and RS's output. In Table 1, the values of the harmonic components' parameters are presented for every test procedure, the symbol  $v$  denotes that the concrete parameter is variable. Every test procedure is comprised of several sub-procedures, each one corresponding to a different value of the variable harmonic parameter. Each sub-procedure is comprised of 12 measurement points which correspond to a different phase shift between fundamental voltage and current,  $U_1$  and  $I_1$ , ranging between  $-90^\circ$  and  $-15^\circ$  and between  $15^\circ$  and  $90^\circ$ , with a step of  $15^\circ$ . No recordings are conducted for  $\phi_1$  between  $-15^\circ$  and  $15^\circ$ , in order for uniform data sets to be presented. Namely, each measurement point corresponds to a  $\phi_1$  value that is  $15^\circ$  phase shifted in relation to adjacent points. If recordings are about to be conducted between  $-15^\circ$  and  $15^\circ$ , then they are supposed to be performed for  $\phi_1 = 0^\circ$ . When the UUT's output is compared with the fundamental reactive power only,  $Q_1$ , in case of harmonically distorted voltages and current, the generated reference power will equal  $0 \text{ VAr}$ . This would lead to a non-defined value for the error result, obtained according to (12).

As described above, results are presented in the form of relative errors, in relation to the reference reactive power, generated by the RS (12). The presented value is calculated as arithmetic mean of 5 recordings, conducted for every measurement point. The whole examination is performed with voltages and currents that equal UUT's nominal values,  $U = 58 \text{ V}$  and  $I = 5 \text{ A}$ .

Only one set of measurements, consisting of 5 recordings, is performed for every measurement point. The result is

presented in the form of 3 mean error values, obtained by comparison between the measurements made by the UUT and the 3 reference reactive power values, for the same distortion conditions: fundamental reactive power only,  $Q_1$ , reactive power calculated according to Budeanu's definition,  $Q_B$ , and reactive power calculated according to the Fryze theory,  $Q_F$ . The results that correspond to a single reference power concept are grouped, on the basis of the harmonic parameter being altered and are presented as "error curves" that depict the UUT's performance in relation to different reference conditions. These "error curves" represent the difference between the measured and the generated reference power due to the implemented measurement algorithm, and will be referred to as "measurement algorithm related error curves".

Table 1. Harmonic parameters in the 5 measurement procedures.

Procedure	$h$	$u_h[\%]$	$i_h[\%]$	$\theta_{uh} [^\circ]$	$\theta_{ih} [^\circ]$
1	5	10	40	0	$v$
2	5	10	40	$v$	60
3	5	10	$v$	0	60
4	5	$v$	40	0	60
5	$v$	10	40	0	60

As illustrated in Fig. 1, the UUT is connected to the RS in a three phase configuration, therefore QRS is supposed to be presented as a three phase reactive power, according to a different power theory. As the measurements are performed in balanced and symmetrical conditions, the three phase reactive power values may be easily obtained from (11), (9), and (7). The three phase fundamental reactive power is calculated by multiplication of (11) with a factor of 3, assuming that voltage and current fundamentals form a symmetrical three phase system. The same conclusion is adopted for calculation of the three phase reactive power according to Budeanu's concept, where beside the fundamentals, high order harmonics in each phase possess the same share and phase shift in relation to fundamentals. The three phase Fryze reactive power is calculated if the three phase active and apparent powers are obtained by multiplying (4) and (6) with a factor of 3, assuming once again symmetrical and balanced conditions for both fundamentals and high order harmonics.

#### 4. RESULTS AND DISCUSSION

Before the differences between the measured and the reference reactive power/energy, in non-sinusoidal conditions, are presented, the intrinsic errors of the UUT, for sine-wave test signals, are presented. These results are supposed to illustrate the actual measuring condition of the UUT and to provide the base for the subsequent validation of the harmonic data. The results corresponding to test voltages and currents of 58 V and 5 A, three phase balanced conditions and phase shifts,  $\varphi$ , in the interval between  $-90^\circ$  and  $-15^\circ$  and between  $15^\circ$  and  $90^\circ$ , are illustrated in Fig. 2.

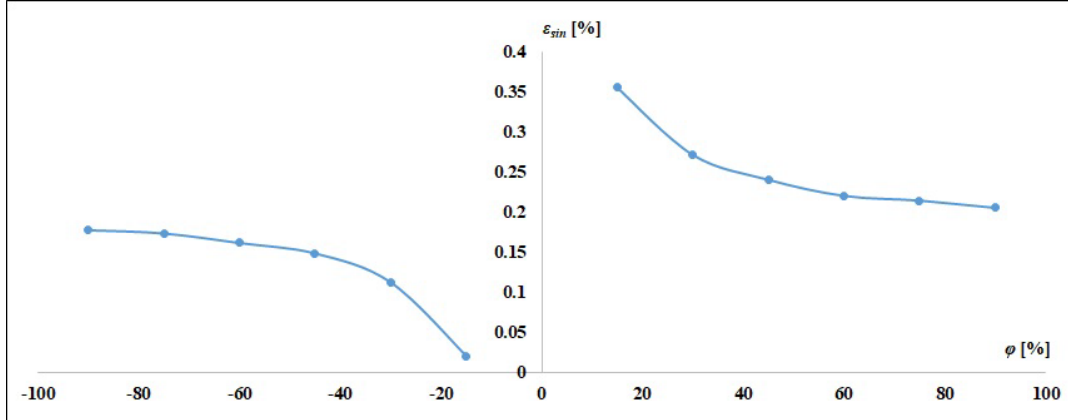


Fig. 2. Intrinsic errors of the UUT for sine wave input signals,  $\epsilon_{sin} = f(\varphi)$ ,  $U = 58$  V and  $I = 5$  A, balanced conditions.

##### A. Comparison between the UUT's measurements and the reference fundamental reactive power, $Q_1$

In the first measurement data set, the UUT's recordings are compared with the fundamental reactive power generated by the RS, i.e.,  $QRS = Q_1$ , (11). The differences between QUUT and QRS are therefore denoted as  $\epsilon_1$ . According to [28], the reactive power is obtained by  $90^\circ$  phase shifting of the voltage signal before its multiplication by the instantaneous current value and it is stated that no harmonic components are recorded. In practice, the separation of fundamental and high order harmonics' power cannot be accomplished by using such a measurement method, because the phase shifting is conducted on a voltage signal that does not possess a pure sinusoidal waveform. The phase shifting of the voltage signal may be accomplished by implementing two solutions [3]. The first method is by using an integrating circuit, that is the analog solution, and the measured power equals:

$$Q_{UUT} = \frac{1}{T} \int_0^T \frac{2\pi}{T} \left[ -\int u(t) dt \right] i(t) dt = \sum_{h=1}^n \frac{U_h I_h \sin \varphi_h}{h}, \quad (13)$$

where  $U_h$ ,  $I_h$ ,  $\varphi_h$  and  $h$  possess the same meaning as described in the second chapter of the manuscript. The second solution for reactive power measurement is based on time shifting of the voltage signal for a quarter period, that is a digitally based solution, and in case of harmonics, QUUT equals:

$$Q_{UUT} = \frac{1}{T} \int_0^T u \left( t + \frac{T}{4} \right) i(t) dt = \sum_{h=1}^n \pm U_h I_h \sin \varphi_h, \quad (14)$$

From the data presented in Fig. 2 it can be concluded that the UUT is in perfect measuring condition. Errors recorded for reference sine-wave conditions are low and are within the meter's accuracy class [28], i.e.,  $\epsilon_{sin} < \pm 1\%$ . In the measurement points that correspond to a high reactive power share in the system, a rather constant performance is recorded,  $\epsilon_{sin}$  equals approximately 0.17% in the capacitive range of  $\varphi$  and 0.2% in the inductive range of  $\varphi$ . For lower phase shifts, a small deviation from the pre-discussed pattern is observed.

where the sign of the  $h$ th reactive power component refers to its power flow orientation. If (14) and (9) are regarded, it can be concluded that this measurement method would result in a measured power equal to the power obtained as proposed by Budeanu. In (13) and (14) the measured power is presented in single phase form, due to a simplified illustration. The three phase measurement is obtained by implementing any of the algorithms on the other two phases as well.

In Fig. 3 and Fig. 4, results from the UUT examination with signals, according to the measurement procedures 1 and 2, are presented, respectively. A general conclusion that can be derived from the two datasets is that the phase shifting of the voltage, for the purpose of reactive power/energy measurement, is based on signals' integration, i.e., on the solution presented in (13). The concrete presumption is provided if obtained "errors" are observed, which are low, i.e., the difference between the measured and the generated power equals approximately  $Q_5/5$ . An additional justification of the measuring principle presented in (13) is that the recorded "measurement algorithm error curves", which are related to a different phase shift of the 5th order components,  $\theta_{i5}$  and  $\theta_{u5}$ , follow a sine-wave pattern with a variable amplitude and a period equal to the period of the harmonic components, i.e.,  $360^\circ/5 = 72^\circ$ . From both figures, it can be seen that the presented dependencies,  $\epsilon_1 = f(\varphi_1)$ , are not symmetrical in relation to the x-axis. This asymmetry is a result of the UUT's intrinsic error intensity, presented in Fig. 2. The difference between the measured power and the generated fundamental power is smaller, when there is a high share of reactive energy in the system, i.e., for phase shifts  $\varphi_1$  between  $\pm 45^\circ$  and  $\pm 90^\circ$ . In these measurement points, maximal deviation of  $\pm 1\%$  is recorded, no matter the initial phase shift of the 5th order harmonics of current or voltage.

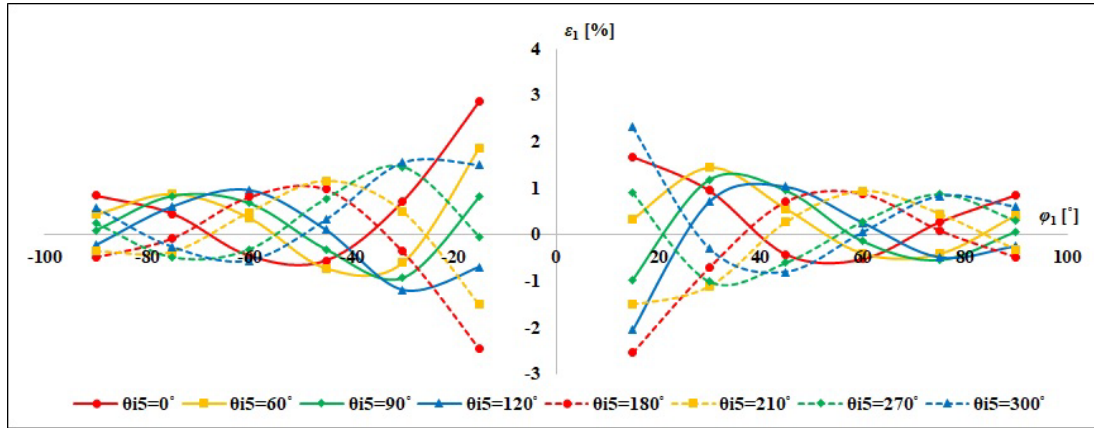


Fig. 3. Difference between  $Q_{UUT}$  and  $Q_{RS} = Q_1$ ,  $\varepsilon_1 = f(\varphi_1)$ , for different values of  $\theta_{i5}$ ,  $u_5[\%] = 10\%$ ,  $i_5[\%] = 40\%$ ,  $\theta_{u5} = 0^\circ$ .

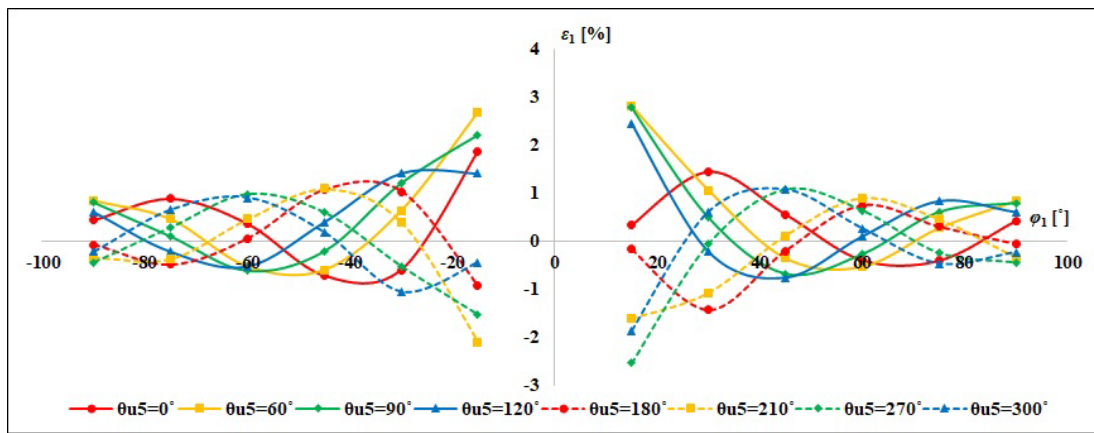


Fig. 4. Difference between  $Q_{UUT}$  and  $Q_{RS} = Q_1$ ,  $\varepsilon_1 = f(\varphi_1)$ , for different values of  $\theta_{u5}$ ,  $u_5[\%] = 10\%$ ,  $i_5[\%] = 40\%$ ,  $\theta_{i5} = 0^\circ$ .

For smaller fundamental phase shifts, i.e., for lower reactive power share in the system, deviations in scale of  $\pm 3\%$  are recorded, and for the most sub-procedures they are present in the measurement points that correspond to  $\varphi_1 = \pm 15^\circ$ . It is expected that these measurement points result in the largest difference between the measured and the generated power, because, for the concrete  $\varphi_1$  values, the ratio  $(Q_5/5):Q_{UUT}$  tends to be maximal. The intrinsic error intensity share is no longer visible, i.e., the overall difference is dominated by the implemented measurement algorithm.

Fig. 5 and Fig. 6 depict the sine wave pattern of the “measurement algorithm error curves” with a period of  $72^\circ$ , for different 5th order current,  $i_5[\%]$ , and 5th order voltage,  $u_5[\%]$ , harmonic share in the signals. There is no phase shift between the curves in both figures, due to the constant  $\theta_{i5}$  and  $\theta_{u5}$  values in all sub-procedures. It can be concluded that the difference between  $Q_{UUT}$  and  $Q_{RS}$  rises linearly with the increase of the harmonic’s share in the test waveforms. The deviation of measured in relation to generated power is more significant in case of a lower reactive power share in the system, i.e., for smaller phase shifts between fundamental components. In both test procedures,  $\varepsilon_1$  values are maximal in the measurement point that correspond to  $\varphi_1 = -15^\circ$ . The maximal difference between  $Q_{UUT}$  and  $Q_1$  in the current harmonic alteration procedure, illustrated in Fig. 5, varies between 1.32%, when  $i_5[\%] = 20\%$ , and 1.88%, when

$i_5[\%] = 40\%$ . In the procedure with variable voltage harmonic, depicted in Fig. 6, the maximal difference equals 0.85% when  $u_5[\%] = 2.5\%$  and 1.88% when  $u_5[\%] = 10\%$ .

In both datasets, illustrated in Fig. 5 and Fig. 6, a mismatch in the sine wave pattern of  $\varepsilon_1 = f(\varphi_1)$  curves exists for low harmonic distortion of the signals. Namely, due to the low intensity of the harmonic power being measured, when  $i_5[\%] < 30\%$  and/or when  $u_5[\%] < 5\%$ , the  $Q_5/5$  measured component is small and it is comparable to the intensity of  $UUT$ ’s intrinsic error, present in sinusoidal conditions, Fig. 2. In some measurement points this interference between the “different sources of error” tends to “amplify” the overall difference between the measured and the generated power, while in others it results in a mutual annulment.

The results from the 5th measurement procedure are illustrated in Fig. 7, as single curves correspond to test voltages and currents that possess harmonic components of different order. In Fig. 7, an additional justification of the meter’s measuring principle is provided. It is expected, regarding (13), that the periods of different “measurement algorithm error curves” are inversely proportional to the harmonic order present in the waveforms, as it is expected to be the case with their amplitudes. As the  $h$  increases,  $Q_{UUT}$  approaches  $Q_1$ , no matter the single component amplitudes and phase shifts, even though their prevalence may result in increased skin effect losses in  $UUT$ ’s circuitry.

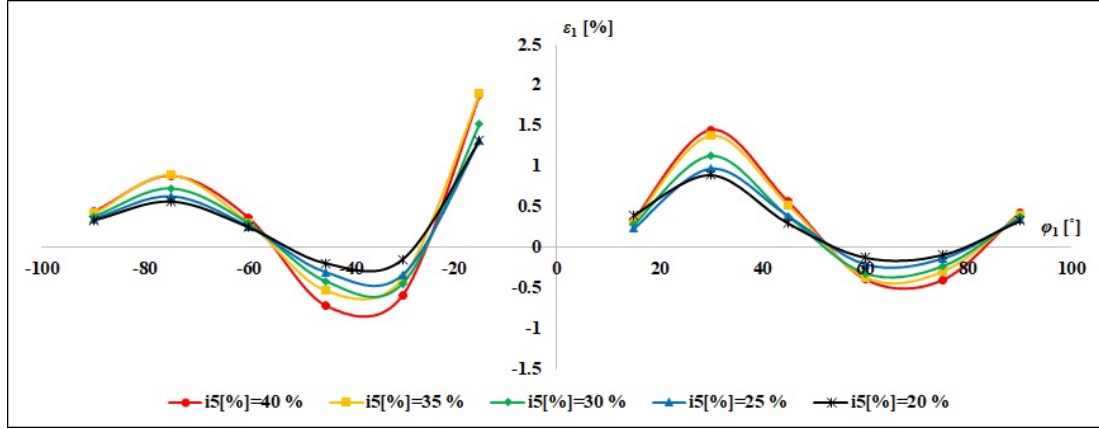


Fig. 5. Difference between  $Q_{UUT}$  and  $Q_{RS} = Q_1$ ,  $\varepsilon_1 = f(\varphi_1)$ , for different values of  $i_s$  [%],  $u_s$  [%] = 10%,  $\theta_{u_s} = 0^\circ$ ,  $\theta_{i_s} = 60^\circ$ .

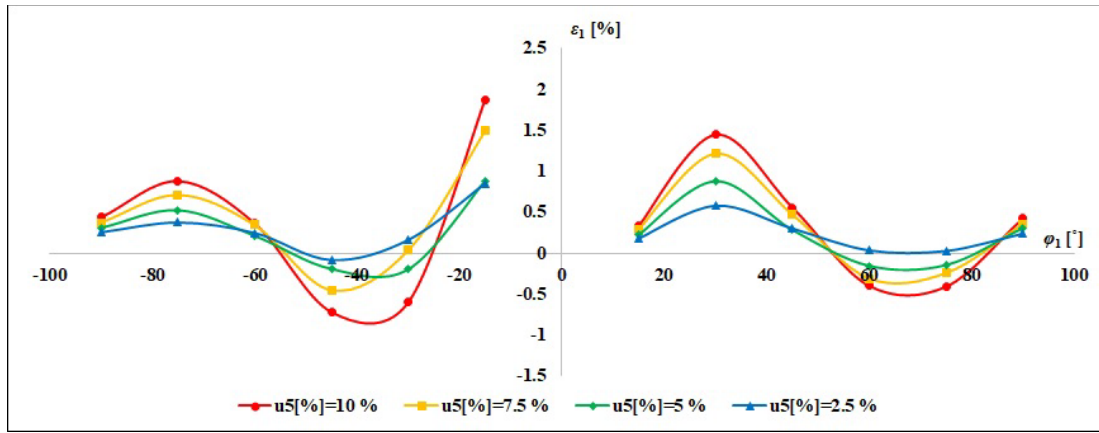


Fig. 6. Difference between  $Q_{UUT}$  and  $Q_{RS} = Q_1$ ,  $\varepsilon_1 = f(\varphi_1)$ , for different values of  $u_s$  [%],  $i_s$  [%] = 40%,  $\theta_{u_s} = 0^\circ$ ,  $\theta_{i_s} = 60^\circ$ .

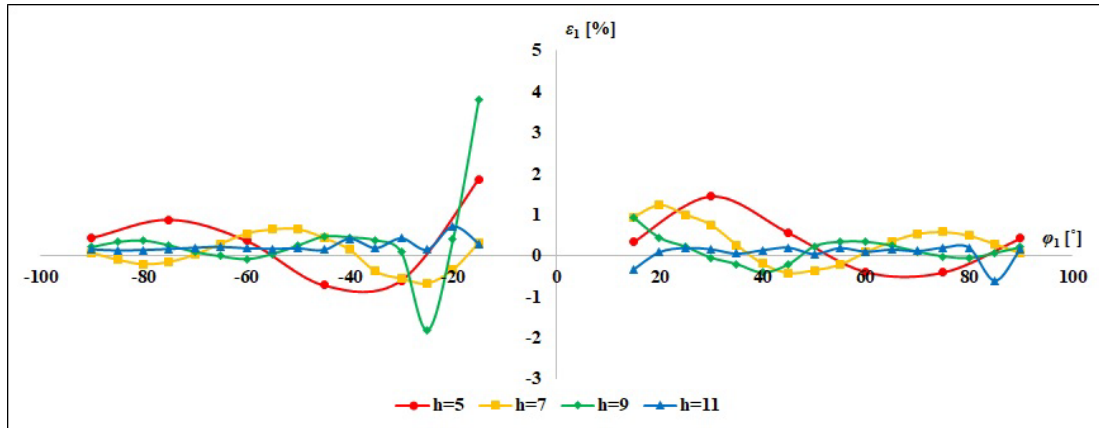


Fig. 7. Difference between  $Q_{UUT}$  and  $Q_{RS} = Q_1$ ,  $\varepsilon_1 = f(\varphi_1)$ , for different harmonic order  $h$ ,  $u_h$  [%] = 10%,  $i_h$  [%] = 40%,  $\theta_{u_h} = 0^\circ$ ,  $\theta_{i_h} = 60^\circ$ .

### B. Comparison between UUT's measurements and the reference Budeanu's reactive power, $Q_B$

Second dataset represents differences between the UUT's measurements and the three phase Budeanu's reactive power,  $Q_B$ . Considering the UUT's measurement algorithm (13), and the generated power, calculated according to Budeanu's concept (9), the relative deviation of the measured power in relation to the generated power, is expected to equal:

$$\varepsilon_B = \frac{\sum_{h=1}^n 3 \frac{U_h I_h \sin \varphi_h}{h} - Q_B}{Q_B} \cdot 100 = - \frac{\sum_{h=2}^n \frac{h-1}{h} Q_h}{Q_B} \cdot 100, \quad (15)$$

where the difference is labeled as  $\varepsilon_B$  in order to denote that the analysis is conducted according to Budeanu's power theory. In the concrete analysis, fundamental power intensity,  $Q_1$ , is much bigger than the high order harmonics' power,  $Q_h$ ,

considering that only one high frequency component is present in both voltage and current signals:

$$U_1 I_1 \sin \varphi_1 \gg U_h I_h \sin \varphi_h, \quad (16)$$

and for every  $h$ , the measurement algorithm related error curves will follow the sine-wave pattern with a period  $h$  times smaller than the period of a 50 Hz signal.

In Fig. 8 and Fig. 9, the difference between QUUT and QRS, in relation to different  $\theta_{i5}$  and  $\theta_{u5}$  values, is presented. The period of single curves equals  $72^\circ$ , i.e., it is 5 times smaller than the period of the 50 Hz signals. From both can be concluded that the deviation amplitudes are approximately 4-5 times larger than the recordings when only the generated Q1 [23] was taken as reference. Such deflections are regarded only as a result of the measurement algorithm, i.e., the intrinsic errors of the UUT, presented in Fig. 2 are neglected. In the  $\varphi_1$  interval between  $\pm 45^\circ$  and  $\pm 90^\circ$ , maximal deviations of  $\pm 6.5\%$  are recorded, no matter the 5th order harmonics initial phase shifts. The  $\theta_{i5}-\theta_{u5}$  phase shift difference results only in displacement of the single parameter alteration curves in relation to the y-axis. For smaller phase shifts between fundamentals, an increase between QUUT and QRS difference is recorded, and it tends to be maximal when  $\varphi_1 = \pm 15^\circ$ . In these measurement points, deviations as high as  $\pm 16\%$  are recorded. The maximal

differences obtained for different  $\varphi_1$  can be regarded as limit values in a broader scenario, even if multiple harmonic components are present in the signals' spectrums, as long as the voltage and current distortion are bounded at 10% and 40%, respectively. It is due to the fact that if more harmonics are considered, components with opposite power flow may exist, and they will tend to cancel each other out.

The measurement algorithm error curves resulting from the alteration of the current and voltage 5th order harmonics share in the waveforms are presented in Fig. 10 and Fig. 11, respectively. They follow the same sine-wave pattern with a period of  $72^\circ$ , as the phase shift difference  $\theta_{i5}-\theta_{u5}$  is fixed at  $60^\circ$ . From both Fig. 10 and Fig. 11, and regarding (15)-(16), it can be concluded that the harmonics' share change results in almost a linear alteration of the deviations' magnitude. The alteration is more noticeable in those measurement points which correspond to a lower reactive power share in the system, i.e., when  $\varphi_1 < \pm 45^\circ$ . Maximal deviation is recorded in the measurement points that correspond to  $\varphi_1 = 15^\circ$ . If the results from the procedure with variable current harmonic are considered, the maximal difference between QUUT and QB varies between  $-4.81\%$ , when  $i_5[\%] = 20\%$ , and  $-9.5\%$ , when  $i_5[\%] = 40\%$ . In case of the voltage 5th order harmonic magnitude alteration procedure it varies between  $-2.48\%$ , when  $u_5[\%] = 2.5\%$ , and  $-9.55\%$ , when  $u_5[\%] = 10\%$ .

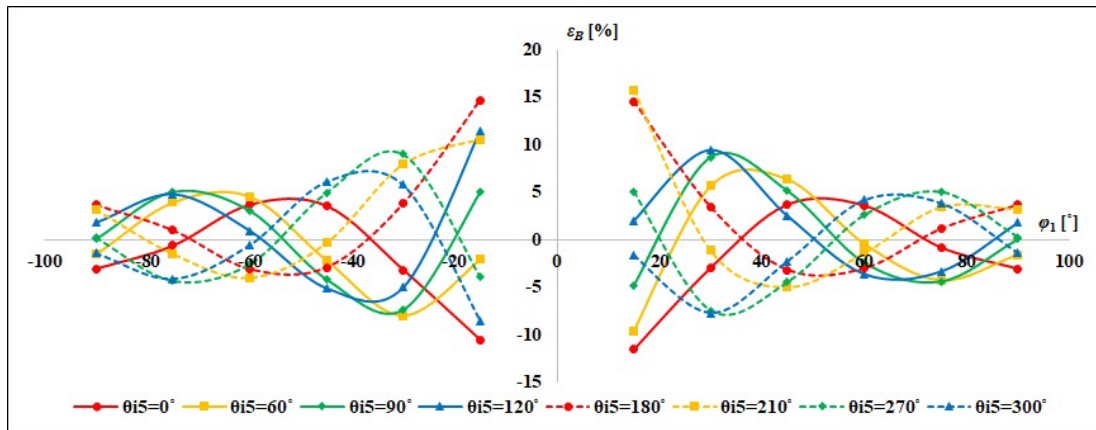


Fig. 8. Difference between  $Q_{UUT}$  and  $Q_{RS} = Q_B$ ,  $\varepsilon_B = f(\varphi_1)$ , for different values of  $\theta_{i5}$ ,  $u_5[\%] = 10\%$ ,  $i_5[\%] = 40\%$ ,  $\theta_{u5} = 0^\circ$ .

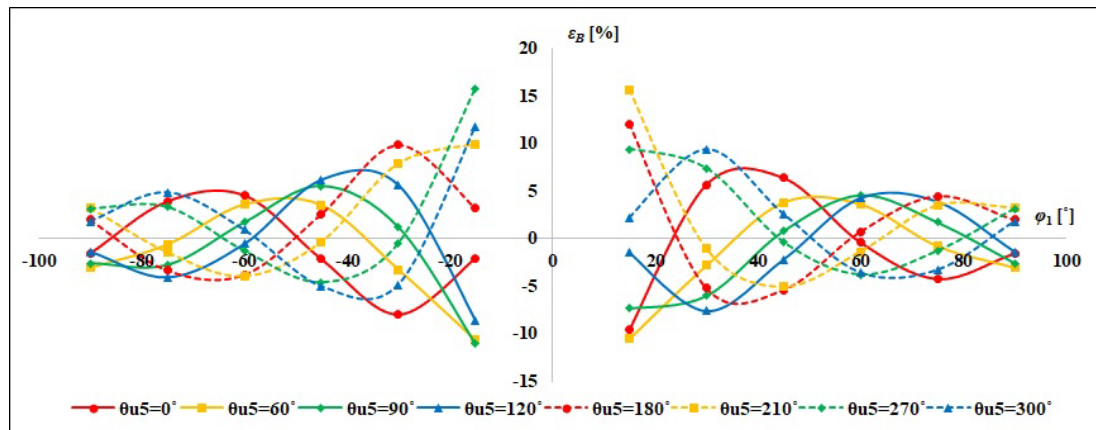


Fig. 9. Difference between  $Q_{UUT}$  and  $Q_{RS} = Q_B$ ,  $\varepsilon_B = f(\varphi_1)$ , for different values of  $\theta_{u5}$ ,  $u_5[\%] = 10\%$ ,  $i_5[\%] = 40\%$ ,  $\theta_{i5} = 60^\circ$ .



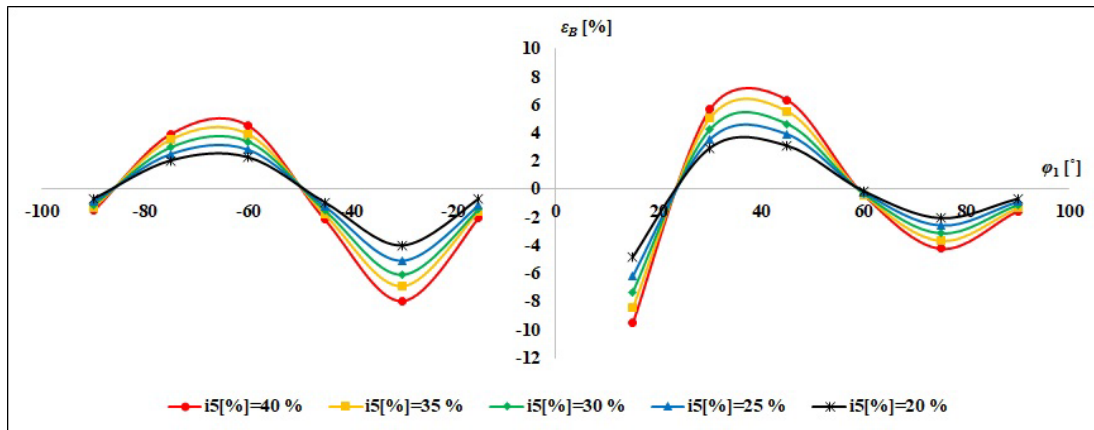


Fig. 10. Difference between  $Q_{UUT}$  and  $Q_{RS} = Q_B$ ,  $\varepsilon_B = f(\varphi_1)$ , for different values of  $i_5[\%]$ ,  $u_5[\%] = 10\%$ ,  $\theta_{u5} = 0^\circ$ ,  $\theta_{i5} = 60^\circ$ .

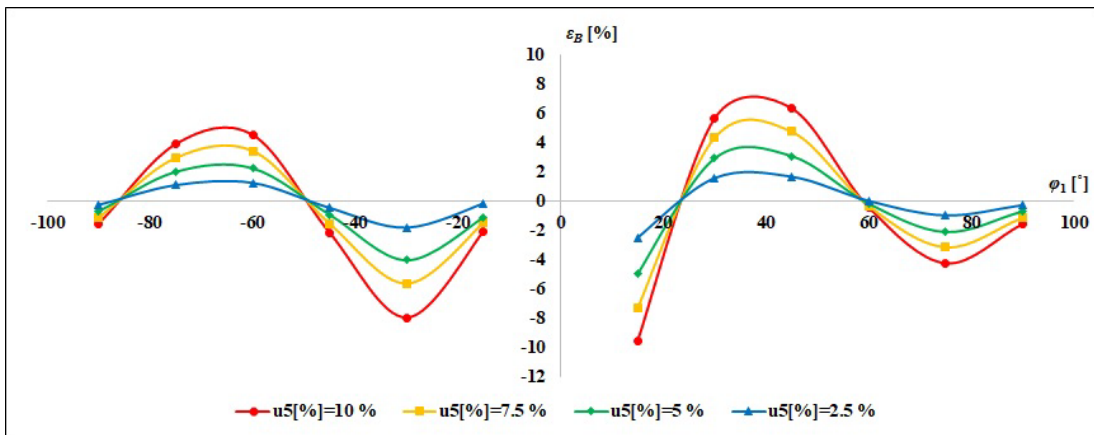


Fig. 11. Difference between  $Q_{UUT}$  and  $Q_{RS} = Q_B$ ,  $\varepsilon_B = f(\varphi_1)$ , for different values of  $u_5[\%]$ ,  $i_5[\%] = 40\%$ ,  $\theta_{u5} = 0^\circ$ ,  $\theta_{i5} = 60^\circ$ .

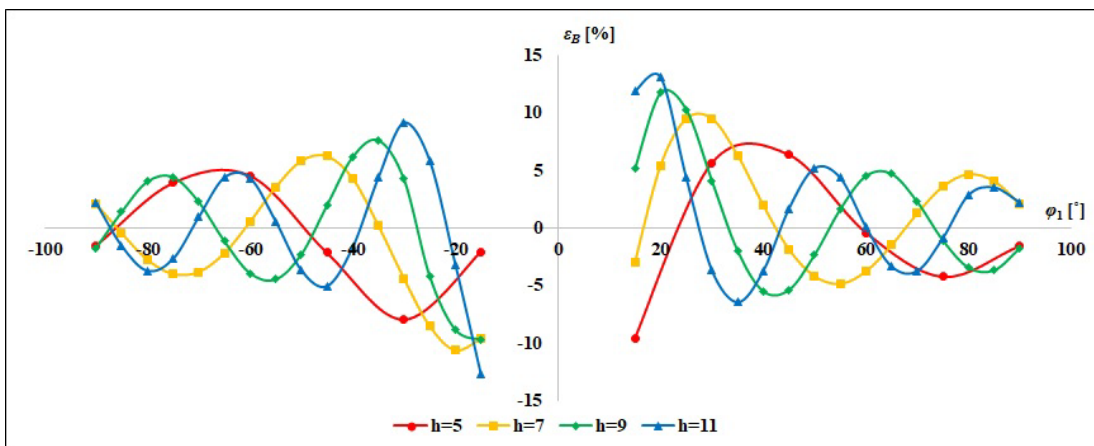


Fig. 12. Difference between  $Q_{UUT}$  and  $Q_{RS} = Q_B$ ,  $\varepsilon_B = f(\varphi_1)$ , for different harmonic order  $h$ ,  $u_h[\%] = 10\%$ ,  $i_h[\%] = 40\%$ ,  $\theta_{uh} = 0^\circ$ ,  $\theta_{ih} = 60^\circ$ .

The verification of the “measurement algorithm error curve” pattern, with a period inversely proportional to the harmonic order, is illustrated in Fig. 12. The period equals  $51.43^\circ$ , when only the 7th order harmonics are considered; it decreases up to  $40^\circ$ , in the 9th order harmonics sub-procedure; while when voltage and current signals possess additional components at 550 Hz, it equals  $32.73^\circ$ . In Fig. 12, a justification is provided about the maximal deviations as well, which are dependent only on the harmonic share in the current and voltage signals. Deviations up to  $\pm 6.4\%$  are

recorded in the  $\varphi_1$  interval between  $\pm 45^\circ$  and  $\pm 90^\circ$  in every sub-procedure, the peak point depends on the function’s period. Maximal differences between QUUT and QB are recorded when  $\varphi_1$  varies between  $\pm 15^\circ$  and  $\pm 30^\circ$ . In the 7th order harmonics sub-procedure  $\varepsilon_{Bmax} = -10.62\%$ , and it is recorded for  $\varphi_1 = -20^\circ$ . If only the 9th order harmonics are present in the waveforms,  $\varepsilon_{Bmax} = 11.76\%$  when  $\varphi_1 = 20^\circ$ , while when signals possess the 11th order harmonics,  $\varepsilon_{Bmax} = 13.12\%$ , for  $\varphi_1 = 20^\circ$ .

C. Comparison between UUT's measurements and the reference Fryze reactive power,  $Q_F$

In the third part of the analysis, the recordings made by the UUT [28] are compared to the reactive power generated by the RS [23], calculated according to the Fryze power theory. If (7), (9) and (11) are compared, it can be concluded that the Fryze power theory results in the highest amount of reactive power share in the system, in relation to the other two approaches, for the same setting of both fundamental components and high order harmonics. Because the reactive power is measured according to (13), the difference between QUUT and QRS is expected to be negative in every measurement point, in all 5 measurement procedures. The results are labeled as  $\epsilon_F$ , to denote that  $Q_{RS} = Q_F$ . The UUT's intrinsic error intensity is expected to be negligible in relation to the overall deviation of the measured power in relation to the generated power, therefore the results will be regarded only from the perspective of the measurement algorithm.

The "measurement algorithm error curves" obtained as a result of the measurement procedures that correspond to alteration of the 5th order harmonics' phase shifts,  $\theta_{i5}$  and  $\theta_{u5}$ , are illustrated in Fig. 13 and Fig. 14, respectively. From both datasets, a justification of the afore-mentioned statement about the negative deviation orientation is provided. The first thing that is noticed from Fig. 13 and Fig. 14 is that  $\epsilon_F$  is little dependent on  $\theta_{i5}$  and  $\theta_{u5}$ , or their difference, when  $\phi_1$  varies

between  $\pm 60^\circ$  and  $\pm 90^\circ$ . The difference between QUUT and QF recorded in these measurement points is comparable to the peak values of the  $\epsilon_B = f(\phi_1)$  curves, illustrated in the previous section of the manuscript, for the same fundamental phase shift interval. The deviation of QUUT in relation to QF varies between -7% and -8% when  $\phi_1 = \pm 90^\circ$  and between -9% and -11%, when  $\phi_1 = \pm 60^\circ$ , depending on different  $\theta_{i5}$  and  $\theta_{u5}$  intensities.

In case of smaller phase shifts, i.e., when  $\phi_1$  is below  $\pm 60^\circ$ , the difference between the measured and the generated power increases significantly and is maximal in the measurement points that correspond to a minimal reactive power share in the system, i.e., when  $\phi_1 = \pm 15^\circ$ . The maximal value varies with alteration of  $\theta_{i5}$ ,  $\theta_{u5}$  or their difference. In the sub-procedures where  $\theta_{i5} - \theta_{u5}$  equals  $0^\circ$  or  $180^\circ$  the "measurement algorithm error curve" is symmetrical in the inductive and capacitive range of  $\phi_1$ . In case of the procedure with variable current harmonic initial phase shift, illustrated in Fig. 13, the afore-mentioned symmetry may be recorded in the results from sub-procedures that correspond to  $\theta_{i5} = 0^\circ$  and  $\theta_{i5} = 180^\circ$ , taking into account that  $\theta_{u5}$  is fixed at  $0^\circ$ . In case of the procedure with variable  $\theta_{u5}$ , illustrated in Fig. 14, the same symmetry may be observed in the sub-procedures that correspond to  $\theta_{u5} = 60^\circ$ , as  $\theta_{i5}$  is fixed at  $60^\circ$ . The maximal deviation equals approximately -43 %, when  $\theta_{i5} - \theta_{u5} = 0^\circ$ , and -50%, when  $\theta_{i5} - \theta_{u5} = 180^\circ$ , for both  $\phi_1 = -15^\circ$  and  $\phi_1 = 15^\circ$ .

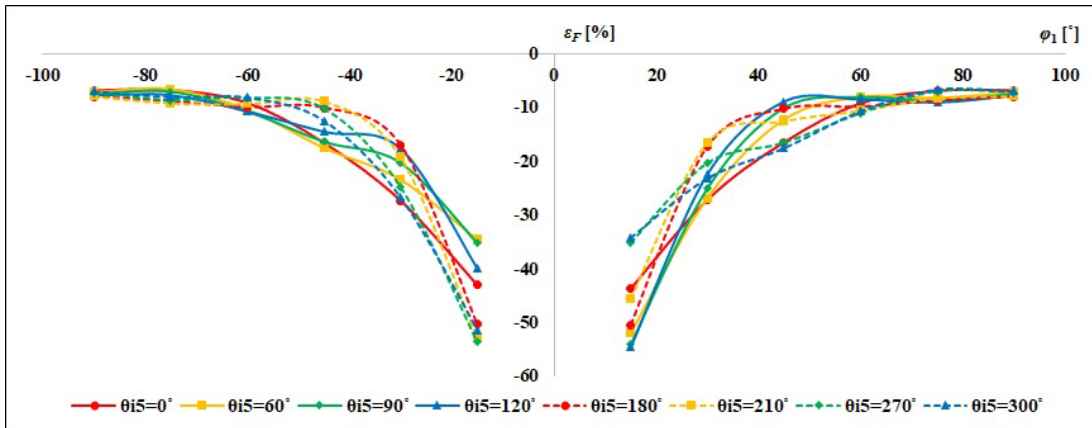


Fig. 13. Difference between  $Q_{UUT}$  and  $Q_{RS} = Q_F$ ,  $\epsilon_F = f(\phi_1)$ , for different values of  $\theta_{i5}$ ,  $u_5[\%] = 10\%$ ,  $i_5[\%] = 40\%$ ,  $\theta_{u5} = 0^\circ$ .

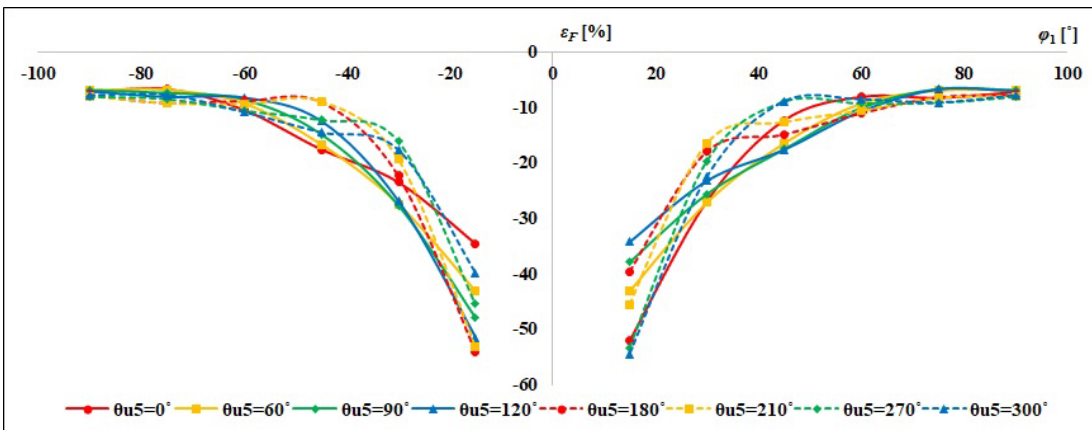


Fig. 14. Difference between  $Q_{UUT}$  and  $Q_{RS} = Q_F$ ,  $\epsilon_F = f(\phi_1)$ , for different values of  $\theta_{u5}$ ,  $u_5[\%] = 10\%$ ,  $i_5[\%] = 40\%$ ,  $\theta_{i5} = 60^\circ$ .

When the phase shift difference  $\theta_{i5}-\theta_{u5}$  is between  $0^\circ$  and  $180^\circ$ , the peak of the  $\varepsilon_F = f(\varphi_1)$  curves is displaced in the inductive range of  $\varphi_1$ . In Fig. 13 this statement is depicted by the results corresponding to  $\theta_{i5}$  being equal to  $60^\circ$ ,  $90^\circ$  and  $120^\circ$  ( $\theta_{u5} = 0^\circ$ ). In Fig. 14, the  $\varepsilon_{Fmax}$  is recorded in the inductive range of  $\varphi_1$ , when  $\theta_{u5}$  equals  $270^\circ$ ,  $300^\circ$  and  $0^\circ$  ( $\theta_{i5} = 60^\circ$ ). On the other hand, when  $\theta_{i5}-\theta_{u5}$  is between  $180^\circ$  and  $360^\circ$ , the maximal difference between QUUT and QRS is recorded in the capacitive range of  $\varphi_1$ . This can be seen from the results illustrated in Fig. 13 that correspond to  $\theta_{i5}$  value of  $210^\circ$ ,  $270^\circ$  and  $300^\circ$ , and from the sub-procedures, illustrated in Fig. 14, in which  $\theta_{u5}$  equals  $90^\circ$ ,  $120^\circ$ ,  $180^\circ$ , and  $210^\circ$ .

In Fig. 15 and Fig. 16, “measurement algorithm error curves” for different  $i_5[\%]$  and  $u_5[\%]$  values, are illustrated, respectively. The two datasets provide additional justification about the relatively constant intensity of the deviations in case of high reactive power share in the system, as well as their sharp alteration, when  $\varphi_1$  is smaller than  $\pm 60^\circ$ . From both figures, the linear dependence between the recorded “errors” and the harmonic’s share is recorded. Because the phase shift difference  $\theta_{i5}-\theta_{u5}$  is constant and it equals  $60^\circ$  in both measurement procedures, the peak point of all curves is recorded in the inductive range of  $\varphi_1$ , i.e., for  $\varphi_1 = 15^\circ$ . The maximal deviation recorded in the current harmonic alteration procedure varies between  $-31.65\%$ , when  $i_5[\%] = 20\%$ , and  $-51.98\%$ , when  $i_5[\%] = 40\%$ . If the results

from the voltage harmonic alteration procedure are analyzed, it can be concluded that the variations of  $\varepsilon_{Fmax}$  lie between  $-47.22\%$ , when  $u_5[\%] = 2.5\%$ , and  $-51.98\%$  when  $u_5[\%] = 10\%$ .

The differences between QUUT and QF, due to harmonic order alteration, are illustrated in Fig. 17. Presented results show small  $\varepsilon_F$  fluctuations in the measurement points that correspond to a maximal reactive power share in the system when  $\varphi_1$  is between  $\pm 70^\circ$  and  $\pm 90^\circ$ . The recorded values in the concrete measurement points do not depend much on the order of harmonics present in the signals and their intensities vary between  $-7.5\%$  and  $-9\%$  in all 4 sub-procedures. The interval corresponding to almost constant deviation intensity is shortening as the harmonic order increases. When the phase shift between fundamental components is between  $\pm 35^\circ$  and  $\pm 70^\circ$ , variable deviation intensities, which oscillate between  $-10\%$  and  $-20\%$ , are recorded. The oscillation period of the curves in this interval is dependent on the order of different harmonic components present in the signals’ spectrums. For lower fundamental phase shifts, the differences between QUUT and QRS increase significantly and are maximal in every sub-procedure, when  $\varphi_1 = 15^\circ$ , equaling approximately  $-52\%$ . The  $\varepsilon_{Fmax}$  is in the inductive range of  $\varphi_1$  due to constant  $\theta_{ih}-\theta_{uh} = 60^\circ$  value, which provides validation of the peak deflection disposition, even when different order harmonics are considered in the voltage and current waveforms.

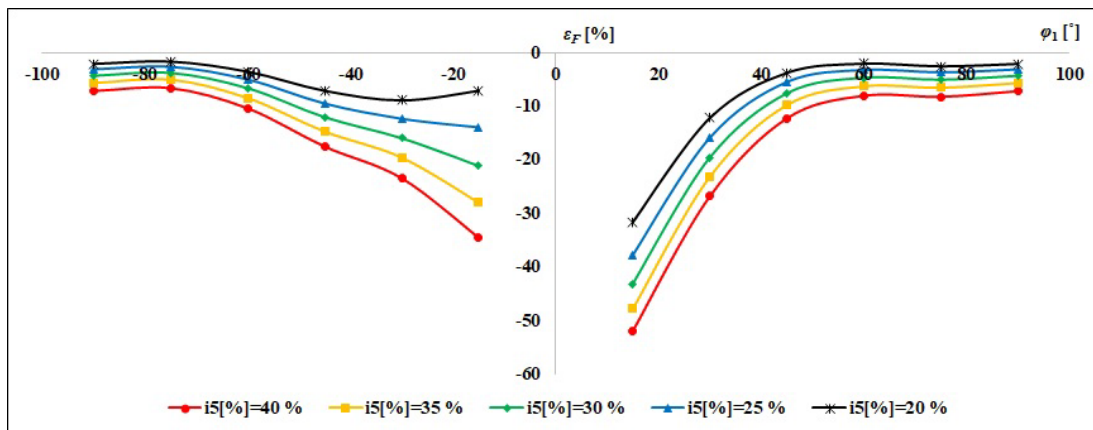


Fig. 15. Difference between  $Q_{UUT}$  and  $Q_{RS} = Q_F$ ,  $\varepsilon_F = f(\varphi_1)$ , for different values of  $i_5[\%]$ ,  $u_5[\%] = 10\%$ ,  $\theta_{u5} = 0^\circ$ ,  $\theta_{i5} = 60^\circ$ .

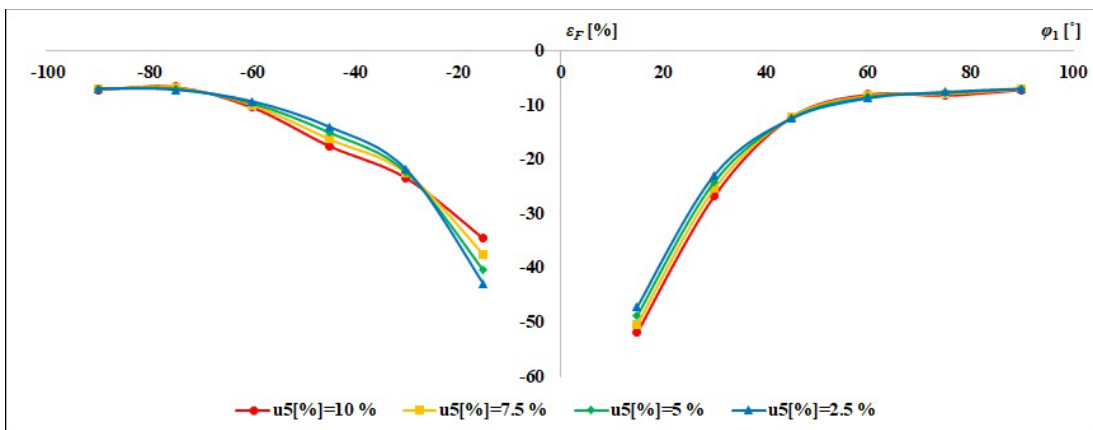


Fig. 16. Difference between  $Q_{UUT}$  and  $Q_{RS} = Q_F$ ,  $\varepsilon_F = f(\varphi_1)$ , for different values of  $u_5[\%]$ ,  $i_5[\%] = 40\%$ ,  $\theta_{u5} = 0^\circ$ ,  $\theta_{i5} = 60^\circ$ .

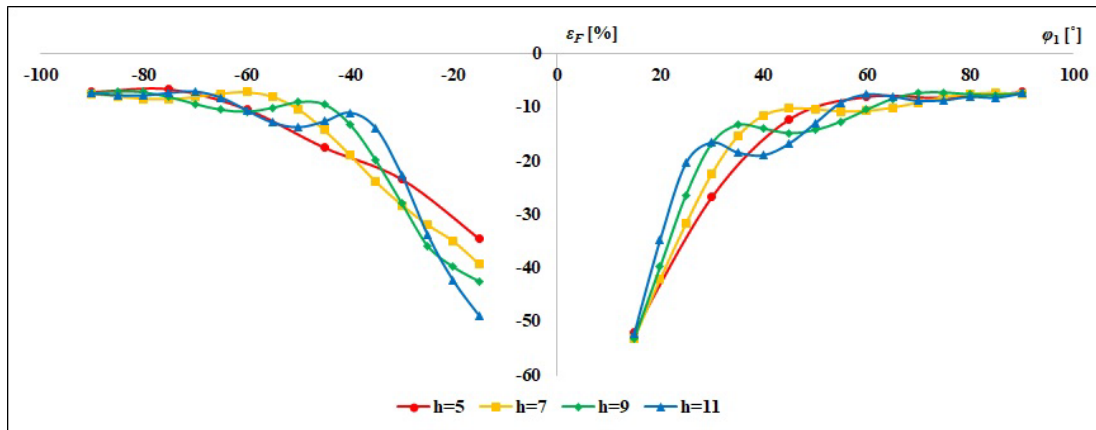


Fig. 17. Difference between  $Q_{UUT}$  and  $Q_{RS} = Q_F$ ,  $\varepsilon_F = f(\varphi_1)$ , for different harmonic order  $h$ ,  $u_h[\%] = 10\%$ ,  $i_h[\%] = 40\%$ ,  $\theta_{uh} = 0^\circ$ ,  $\theta_{ih} = 60^\circ$ .

## 5. CONCLUSION

In the manuscript, an analysis of reactive energy electricity meter's performance, from the perspective of its measurement algorithm, in relation to different harmonic components' parameters values and different power theories adopted, is performed. The analysis is conducted starting from real measurements made in an accredited calibration laboratory. The measurements are performed with waveforms standardized for active energy electricity meter examination, as no standardized protocols for reactive power/energy instrument testing in case of harmonics are provided. A total of 5 procedures is implemented, each one corresponding to different harmonic parameter alteration. From every procedure 3 measurement datasets are obtained, in each, the UUT's output is compared to the generated reference power, calculated according to a different power definition.

The UUT's measuring principle, which is not explicitly declared by the manufacturer, is determined by using the results from the first dataset, when  $QRS = Q_1$ . The results lead to a conclusion that the UUT measuring principle is based on a  $90^\circ$  phase shift of the input voltages, by means of an integrating circuit. "Measurement algorithm error curves", obtained by different harmonic parameter alterations, follow the sine-wave pattern of  $\varphi_1$ , with a period inversely proportional to the harmonic order,  $h$ . If only the 5th order harmonics with 10% voltage and 40% current distortion are present in the waveforms, the difference between  $QUUT$  and  $QRS$  is small, below  $\pm 1\%$ , when  $\varphi_1$  equals between  $\pm 45^\circ$  and  $\pm 90^\circ$ , and below  $\pm 3\%$  for smaller phase shifts. If higher order harmonics with the same share are considered, even smaller deviations are recorded, due to the inverse proportionality of  $h$  and single  $\varepsilon_1 = f(\varphi_1)$  curves amplitudes.

If the UUT's readings are compared to the generated power, calculated according to Budeanu's concept, an increase of the deviations in measurements is recorded. Single error curves follow the sine-wave pattern of  $\varphi_1$ , with a period inversely proportional to the order of harmonics present in the signals' waveforms. The differences between  $QUUT$  and  $QRS$  are 4 to 5 times larger than the values obtained from the first dataset. Maximal deviations up to  $\pm 6.5\%$  are recorded in case of high reactive power share in the system, i.e., when  $\varphi_1$  is between  $\pm 45^\circ$  and  $\pm 90^\circ$ , while the difference between  $QUUT$  and  $QB$  is up to  $\pm 16\%$  for smaller

phase shifts. The concrete values correspond to fixed voltage and current distortion of 10% and 40%, respectively, and variable harmonic order and phase shifts. For lower harmonic share, a linear decrease in the results presented is recorded.

In the third measurement dataset, the UUT's performance is related to the Fryze reactive power. The recorded deviations in this dataset are negative, for any value of the harmonic parameter being altered. The difference between the measured and the generated power is rather constant, between  $-7\%$  and  $-11\%$  in the  $\varphi_1$  interval between  $\pm 60^\circ$  and  $\pm 90^\circ$ , if only the 5th order harmonics are regarded. For smaller  $\varphi_1$  values, error results increase significantly, reaching maximal magnitudes between  $-43\%$  and  $-53\%$ . The shape of the  $\varepsilon_F = f(\varphi_1)$  is not affected by the alteration of harmonic share in the signals, as is the case if components of different order are considered.

## REFERENCES

- [1] Directive of European Parliament and of the Council. (2014). *EU Directive on Measuring Instruments (MID)*. 2014/32/EU. <https://eur-lex.europa.eu/legal-content/EN/TXT/?uri=CELEX:32014L0032>
- [2] International Organization of Legal Metrology (OIML). (2012). Active electrical energy meters. Part 1: Metrological and technical requirements. Part 2: Metrological controls and performance tests. OIML R 46-1/-2. [https://www.oiml.org/en/files/pdf\\_r/r046-1-2-e12.pdf](https://www.oiml.org/en/files/pdf_r/r046-1-2-e12.pdf)
- [3] Cataliotti, A., Cosentino, V., Lipari, A., Nuccio, S. (2010). On the methodologies for the calibration of static electricity meters in the presence of harmonic distortion. In *17th Symposium IMEKO TC 4, 3rd Symposium IMEKO TC 19 and 15th IWADC Workshop Instrumentation for the ICT Era*, 4, 8-10. <https://www.imeko.org/publications/tc4-2010/IMEKO-TC4-2010-072.pdf>
- [4] British Standards Institution (BSI). (2018). *Electricity metering equipment (a.c.) Part 1: General requirements, tests and test conditions – Metering equipment (class indexes A, B and C)*. EN 50470-1:2006+A1:2018.

- [5] British Standards Institution (BSI). (2018). *Electricity metering equipment (a.c.) Part 2: Particular requirements - Electromechanical meters for active energy (class indexes A and B)*. EN 50470-2:2006+A1:2018.
- [6] British Standards Institution (BSI). (2018). *Electricity metering equipment (a.c.) Part 3: Particular requirements - Static meters for active energy (class indexes A, B and C)*. EN 50470-3:2006+A1:2018.
- [7] Olencki, A., Mróz, P. (2014). Testing of energy meters under three-phase determined and random nonsinusoidal conditions. *Metrology and Measurement Systems*, 21 (2), 217-232.  
<http://dx.doi.org/10.2478/mms-2014-0019>
- [8] Masri, S., Khairunaz, M.D., Mamat, M.N. (2019). Study of electronic energy meter performance under harmonics current condition. In *10th International Conference on Robotics, Vision, Signal Processing and Power Applications*. Springer, LNEE, 547, 449-456.  
[https://doi.org/10.1007/978-981-13-6447-1\\_57](https://doi.org/10.1007/978-981-13-6447-1_57)
- [9] Bartolomei, L., Cavaliere, D., Mingotti, A., Peretto, L., Tinarelli, R. (2020). Testing of electrical energy meters subject to realistic distorted voltages and currents. *Energies*, 13 (8), 2023.  
<https://doi.org/10.3390/en13082023>
- [10] Morva, G., Volokhin, V., Diahovchenko, I., Čonka, Z. (2017). Analysis of the impact of nonlinear distortion in voltage and current curves on the errors of electric energy metering devices. In *2017 IEEE First Ukraine Conference on Electrical and Computer Engineering (UKRCON)*. IEEE, 528-533.  
<https://doi.org/10.1109/UKRCON.2017.8100296>
- [11] Bartolomei, L., Cavaliere, D., Mingotti, A., Peretto, L., Tinarelli, R. (2019). Testing of electrical energy meters in off-nominal frequency conditions. In *2019 IEEE 10th International Workshop on Applied Measurements for Power Systems (AMPS)*. IEEE, 1-6.  
<https://doi.org/10.1109/AMPS.2019.8897781>
- [12] Ferrero, A., Faifer, M., Salicone, S. (2009). On testing the electronic revenue energy meters. *IEEE Transactions on Instrumentation and Measurement*, 58 (9), 3042-3049.  
<https://doi.org/10.1109/TIM.2009.2016821>
- [13] Raza, S.S., Ahmad, M., Perveiz, M.S. (2014). Performance of energy meters under harmonic generating environment. *Science International (Lahore)*, 26 (5), 2063-2069.
- [14] Demerdziev, K., Dimchev, V. (2021). Analysis of errors in active power and energy measurements under random harmonic distortion conditions. *Measurement Science Review*, 21 (6), 168-179.  
<https://doi.org/10.2478/msr-2021-0023>
- [15] Barbaro, P.V., Cataliotti, A., Cosentino, V., Nuccio, S. (2006). Behavior of reactive energy meters in polluted power systems. In *XVIII IMEKO World Congress: Metrology for a Sustainable Development*. IMEKO, 172 (2).  
<https://www.imeko.org/publications/wc-2006/PWC-2006-TC4-060u.pdf>
- [16] International Electrotechnical Committee (IEC). (2020). *Electricity metering equipment - Particular requirements - Part 23: Static meters for reactive energy (classes 2 and 3)*. IEC 62053-2:2020.
- [17] Institute of Electrical and Electronics Engineers (IEEE). (2010). *Definitions for the Measurement of Electric Power Quantities Under Sinusoidal, Nonsinusoidal, Balanced, or Unbalanced Conditions*. IEEE Std. 1459:2010. <https://doi.org/10.1109/IEEESTD.2010.5439063>
- [18] Berrisford, A.J. (2018). The harmonic impact project-IEEE-1459 power definitions trialed in revenue meters. In *2018 IEEE International Instrumentation and Measurement Technology Conference (I2MTC)*. IEEE, 1-5. <https://doi.org/10.1109/I2MTC.2018.8409542>
- [19] Zobaa, A.F. (2011). *Power Quality: Monitoring, Analysis and Enhancement*. Rijeka, Croatia: IntechOpen, ISBN 978-953-307-330-9.
- [20] Santoso, S., McGranaghan, M.F., Dugan, R.C., Beaty, H.W. (2012). *Electrical Power Systems Quality*, 3rd Edition. McGraw-Hill, ISBN 978-0071761550.
- [21] Grady, M. (2006). *Understanding power system harmonics*. University of Texas, Austin, Texas, USA.
- [22] Rangelov, Y. (2014). Overview on harmonics in the electrical power system. In *International Scientific Symposium: Electrical Power Engineering 2014*. Electrical Engineering Faculty, Technical University of Varna, Varna, Bulgaria, 63-70. ISBN 978-954-20-0497-4.
- [23] Calmet, LtD. (2013). *300 three phase power calibrator and power engineering apparatus testing*. User's manual and extended specifications.
- [24] Balci, M.E., Hocaoglu, M.H. (2004). Comparison of power definitions for reactive power compensation in nonsinusoidal conditions. In *2004 11th International Conference on Harmonics and Quality of Power*. IEEE 519-524.  
<https://doi.org/10.1109/ICHQP.2004.1409408>
- [25] International Organization for Standardization (ISO). (2017). *General requirements for the competence of testing and calibration laboratories*. ISO/IEC 17025.
- [26] Demerdziev, K., Cundeve-Blajer, M., Dimchev, V., Srbinovska, M., Kokolanski, Z. (2018). Improvement of the FEIT laboratory of electrical measurements best CMC through internationally traceable calibrations and inter-laboratory comparisons. In *XIV International Conference ETAI*. Struga, North Macedonia.
- [27] Demerdziev, K., Cundeve-Blajer, M., Dimchev, V., Srbinovska, M., Kokolanski, Z. (2019). Defining an uncertainty budget in electrical power and energy reference standards calibration. In *IEEE EUROCON 2019-18th International Conference on Smart Technologies*. IEEE, 1-6.  
<https://doi.org/10.1109/EUROCON.2019.8861600>
- [28] Landys+Gyr. (2017). *ZMD400AT/CT E650 Series 4*. User manual.

Received April 28, 2022  
Accepted December 20, 2022